Neurochemistry International 129 (2019) 104471

Contents lists available at ScienceDirect

Neurochemistry International

journal homepage: www.elsevier.com/locate/neuint

Effect of phosphodiesterase (1B, 2A, 9A and 10A) inhibitors on central nervous system cyclic nucleotide levels in rats and mice

Jie Chen[*,1], Douglas Zook[2], Lindsay Crickard[3], Ali Tabatabaei[**,4]

Dart NeuroScience, LLC, 12278 Scripps Summit Drive, San Diego, CA, 92131, United States

ARTICLE INFO

Keywords:
Phosphodiesterase inhibitor
Rodent CNS
Biomarkers
Cyclic adenosine monophosphate
Cyclic guanosine monophosphate
Synergistic effect

Chemical compounds studied in this article:
PF-4447943 (PubChem CID: 25115162)
MP10 or PF-2545920 (PubChem CID: 11581936)

ABSTRACT

Phosphodiesterase (PDE) inhibition has been broadly investigated as a target for a wide variety of indications including central nervous system (CNS) disorders. Cyclic nucleotide (cNT) changes within associated tissues may serve as a biomarker of PDE inhibition. We recently developed robust sample harvesting and bioanalytical methods to quantify cNT levels in rodent brain and cerebrospinal fluid (CSF). Herein, we report on the application of those methods to study rodent species-specific and rodent brain region-specific cNT changes following individual or concomitant PDE inhibitor administration.

Male Sprague Dawley (Crl:CD® [SD]) rats were dosed subcutaneously (sc) with a PDE1B inhibitor (DNS-0056), a PDE2A inhibitor (PF-05180999), a PDE9A inhibitor (PF-4447943), and a PDE10A inhibitor (MP10), each at a single dose of 10 or 30 mg/kg, or concomitantly with all 4 inhibitors at 10 mg/kg each. Male Carworth Farms (Crl:CF1 ®[CF-1]) mice were dosed intraperitoneally (ip) with the four individual inhibitors at a single dose of 10 mg/kg or concomitantly with all 4 inhibitors at 10 mg/kg each. The doses studied are generally adequate for affecting measurable cNT levels in the tissues of interest and were thereby chosen for this investigation. Measured 3′,5′-cyclic adenosine monophosphate (cAMP) changes were generally statistically insignificant in the brain, striatum and CSF after administration of the aforementioned PDE inhibitors. However, the levels of 3′,5′-cyclic guanosine monophosphate (cGMP) increased in both rat and mouse striatum (2.2-, 2.1- and 1.7-fold and 6.4-, 2.8- and 1.7-fold, respectively) after PDE2A, 9A, and 10A inhibitor dosing. In all cases, the cNT changes followed the same trend in the brain, striatum and CSF after PDE inhibitor dosing and dose response was observed in rats. Concomitant treatment with PDE1B, PDE2A, PDE9A and PDE10A inhibitors resulted in a 4.4- and 36.7-fold increase of cGMP in rat and mouse striatum. The drug exposures after concomitant treatment were also higher than in the individual inhibitor-treated animals. cGMP enhancement observed could be due to synergistic effects, though an additive effect of the combined inhibitor concentrations may also contribute.

1. Introduction

Phosphodiesterases (PDEs) have been evaluated as a target for many therapeutic areas due to their critical role in regulating intracellular 3′,5′-cyclic adenosine monophosphate (cAMP) and/or 3′,5′-cyclic guanosine monophosphate (cGMP) levels (Ahmad et al., 2015). Clinically, abnormally low cyclic nucleotide (cNT) levels in cerebrospinal fluid (CSF) have been associated with Alzheimer's disease, Schizophrenia, Creutzfeldt-Jakob disease and other neurodegenerative diseases (Keravis and Lugnier, 2012; Oeckl et al., 2012).

Cyclic AMP and cGMP, respectively, are synthesized by adenosine cyclase (AC) and guanylyl cyclase (GC) and are degraded by cNT PDEs or removed from the cell by efflux transporters such as multidrug resistance-associated protein 4 (MRP4). PDEs are the only family of enzymes that hydrolyze the 3' cyclic phosphate bonds of cAMP and/or cGMP thereby terminating their function. The maximum rate of cNT

* Corresponding author.
** Corresponding author.
E-mail addresses: chenjie_ca@hotmail.com, Jchen@arcusbio.com (J. Chen), dzook@metacrine.com (D. Zook), lcrickard@neurocrine.com (L. Crickard), alit@vividion.com (A. Tabatabaei).
[1] Present address: Arcus BioSciences, 3928 Point Eden Way, Hayward, California; 94545, US.
[2] Present address: Metacrine, Inc. 3985 Sorrento Valley Blvd. San Diego, California, 92121, US.
[3] Present address: Neurocrine Biosciences, Inc. 12780 El Camino Real, San Diego, California 92130, US.
[4] Present address: Vividion Therapeutics, 5820 Nancy Ridge Dr., San Diego, California, 92121, US.

https://doi.org/10.1016/j.neuint.2019.104471
Received 29 January 2019; Received in revised form 14 May 2019; Accepted 16 May 2019
Available online 20 May 2019
0197-0186/

hydrolysis by PDE is approximately 10 times faster than that of synthesis by cyclase (Beavo and Brunton, 2002; Schmidt, 2010), therefore PDEs are effective regulators of the cNTs. Increased intracellular levels of cAMP and/or cGMP lead to alteration of cAMP-dependent protein kinase (PKA) and/or cGMP-dependent protein kinase (PKG) activities with subsequent changes in cellular function. This process is amplified as a single intracellular messenger molecule leading to the synthesis of multiple copies of cAMP and/or cGMP, and each molecule of cAMP or cGMP in turn, activates multiple copies of PKA or PKG.

It is well established that the cNTs execute their function within microcompartments in the cell. The scope of cNT compartmentalization starts from its formation: ligand binding to specific G protein-coupled receptors (GPCRs) selectively activates specific ACs or GCs resulting in the generation of cAMP or cGMP in a limited intracellular space. PDEs proximal to this space regulate the duration and the spatial distribution of cAMP or cGMP facilitating the formation of a transient, localized cAMP or cGMP 'cloud'. A-kinase anchoring proteins (AKAPs), tether PKAs to specific subcellular locations filled with a cAMP 'cloud' and activate PKA. The activated PKA results in the phosphorylation of local substrates. Such spatial-temporal dynamic changes of cAMP in the living cell have been detected by modern fluorescence resonance energy transfer (FRET) (Evellin et al., 2004).

The PDE superfamily is comprised of at least 12 isoenzymes with over 50 isoforms that are encoded by 21 genes. Some of the PDE isoenzymes are cAMP-specific (eg, PDE4, PDE7 and PDE8), some are cGMP-specific (eg, PDE5, PDE6 and PDE9) and some are dual-specific (eg, PDE1, PDE2, PDE3, PDE10 and PDE11) (Ke et al., 2011; Menniti et al., 2006). Each PDE isoenzyme and variant is localized to specific tissues and cell types and performs specific physiological functions. Among those PDE isoenzymes, PDE1, PDE2, PDE4, PDE7, PDE9 and PDE10 are found in the rat brain (Kelly et al., 2014) (Fig. 1). The striatum is a region rich in PDEs, especially PDE1, PDE2 and PDE10 (Kelly et al., 2014; Schmidt, 2010). A synergistic effect has been observed in lung after concomitant administration of PDE3, PDE4 and PDE5 inhibitors for the treatment of pulmonary vasodilatory response (Schermuly et al., 1999); and for activation of brown adipose tissue after concomitant administration of PDE3 and PDE4 inhibitors (Kraynik et al., 2013). It was observed that concomitant administration of PDE2 and PDE10 inhibitors enhanced cGMP levels in rat brain (Megens et al., 2014), however, little information is available regarding compound exposure after concomitant administration. The apparent synergistic effect could be a result of true synergy, an increase of inhibitor concentrations, or a combination of both.

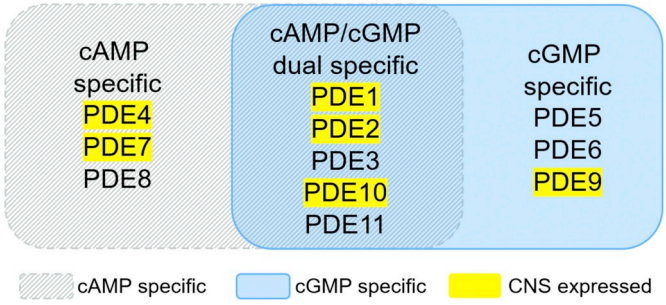

Fig. 1. Substrate specificity and CNS expression of PDE isoenzymes.

PDEs have been evaluated as a potential drug target for over four decades. To date, the clinical success of PDE inhibition is limited to a few peripheral indications, however the association of cNT modulation and cognitive function is well-established (Schmidt, 2010). Accordingly, there is a surge in identifying CNS drugs targeting PDE inhibition and many new drug candidates are undergoing both preclinical and clinical investigation. For this study, we chose an internally developed advanced lead (DNS-0056), and three reference compounds (PF-05180999, PF-4447943 and MP10) with varied PDE selectivity profiles (Fig. 2). DNS-0056 is a PDE1B inhibitor efficacious in the rat novel object recognition (NOR) model at a dose of 0.3 mg/kg (Dyck et al., 2017); PF-05180999 is a PDE2A inhibitor that entered clinical trials (Helal et al., 2017); and PF-4447943 is a potent and selective PDE9A inhibitor that also entered clinical trials (Kleiman et al., 2012) as did MP10, a very potent and selective PDE10A inhibitor (Grauer et al., 2009). The potency/brain tissue binding as well as the physicochemical properties of the above PDE inhibitors are listed in Table 1 and Table 1s respectively. The PDEs investigated in this study (PDE1, PDE2, PDE9 and PDE10) include all the PDEs expressed in the brain and all modulate cGMP. Striatum is a tissue rich in PDE expression.

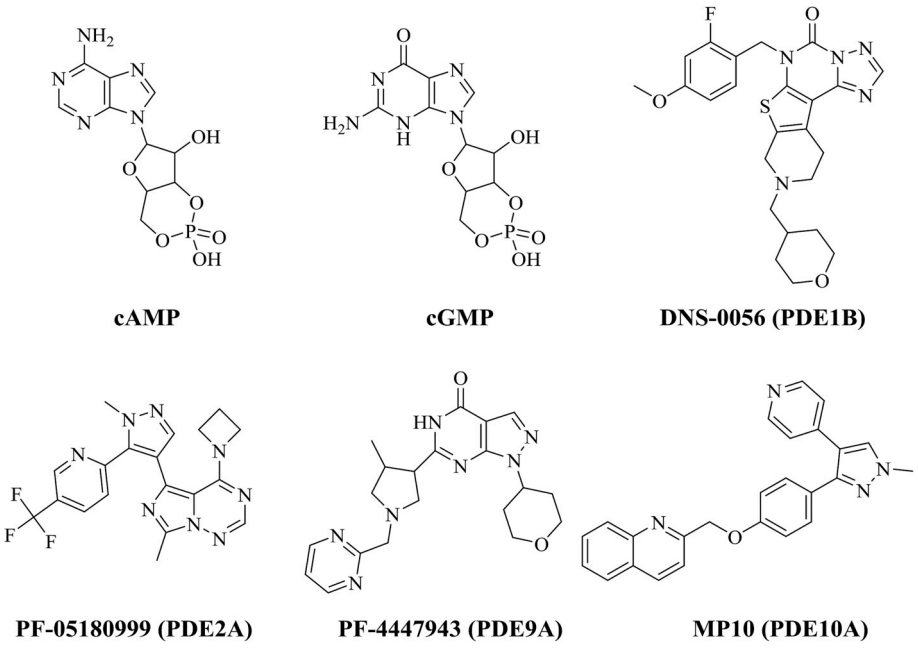

Fig. 2. Chemical Structures of Two cNTs (cAMP and cGMP) and Four PDE Inhibitors.

Table 1
Potency (μM) and brain binding of the inhibitors tested.

Compound	PDE1B (EC_{50})	PDE2A (EC_{50})	PDE9A (EC_{50})	PDE10A (EC_{50})	Rat brain binding (f_u)
DNS-0056	0.04	6.03	75.0	0.71	1.6
PF-05180999	75.0	0.0004	NA	5.5	12.7
PF-4447943	26.6	75.0	0.007	75.0	36.8
MP10	75.0	14.4	NA	0.0006	0.1

2. Materials and method

2.1. Reagents

DNS-0056 (a PDE1B inhibitor) and PF-05180999 (a PDE2A inhibitor) were synthesized in-house; PF-4447943 (a PDE9A inhibitor) was obtained from Synnovator, Inc. (NC, United States [US]); MP10 (a PDE10A inhibitor) was obtained from Wuxi AppTec (Shanghai, China); 3′,5′-cyclic adenosine-$^{13}C_5$ monophosphate ($^{13}C_5$-cAMP) and 3′,5′-cyclic guanosine-$^{13}C^{15}N_2$ monophosphate ($^{13}C^{15}N_2$-cGMP) were obtained from Toronto Research Chemicals, Inc. (North York, Ontario, Canada), 3′,5′-cyclic adenosine-monophosphate (cAMP) sodium (Na) salt, 3′,5′-cyclic guanosine-monophosphate (cGMP) Na salt, 3′,5′-cyclic inosine monophosphate (cIMP) Na salt, carbamazepine, carboxymethyl cellulose (CMC), formic acid (FA; approximately 98%), perchloric acid (PCA), dimethyl sulfoxide (DMSO) and acetonitrile (ACN) were purchased from Sigma-Aldrich (MO, US).

2.2. Dose administration and tissue collection

All animals were group housed under standard vivarium conditions on a 12-h light-dark cycle with food and water provided *ad libitum*. The animals were handled and cared for according to Dart NeuroScience Institutional Animal Care and Use Committee (IACUC) approved protocols and were acclimated for at least 48 h prior to dosing.

Male Sprague Dawley (Crl:CD® [SD]) rats (200–250 g) were obtained from Charles River Laboratories (CRL; Hollister, CA, US). The animals (n = 6/group) were administered 4 PDE inhibitors, or vehicle control, individually at a dose of 10 or 30 mg/kg subcutaneously (sc) or concomitantly with all 4 inhibitors at a dose of 10 mg/kg each. Individual inhibitors or a cocktail of the four inhibitors were formulated in a mixture of N-methyl-2-pyrrolidone (NMP), polyethylene glycol 400 (PEG400) and water (10:40:50). One hour after administration, the animals were sacrificed by brain-focused microwave irradiation (Muromachi MMW-05 with a WJR-L water-jacketed rat restrainer; 1.4 s at 5 kW). Microwave irradiated rats were then decapitated and the cranium was removed to expose the irradiated brain for harvesting. Using the flat end of a spatula, an approximate 1 mm depth incision was made vertically to the midline of the brain and the cortex was carefully removed. Under the cortex on both sides of the frontal lobe of the brain, the striatum was identified as a mung bean shape approximately 2 mm in diameter. Using the sharp end of a spatula, striatum was carefully separated by following the striatal walls with the lateral ventricles and the corpus callosum. The striatum and the remainder of the brain tissues (including the cerebellum and brain stem) were individually weighed and transferred to 1 mL cryotubes and placed on dry ice until the end of the procedure. Samples were then stored frozen (−80 °C) until bioanalysis.

Supplemental groups of animals were dosed sc with the four inhibitors, either individually or concomitantly, at 10 mg/kg for CSF collection. Rats were anesthetized with inhalant Isoflurane. After confirming the depth of anesthesia with a toe pinch, a terminal blood sample was collected (1 mL) by cardiac puncture with a 18 G needle. Using a scalpel, a vertical incision was made in the scalp to expose the muscle tissues. A deeper incision was made to expose the cranium, using the back of the scalpel blade to tease away the muscle tissues to expose the cisterna magna. The cisterna magna is located at the base of the cranium. Using a 27 × ½ G winged needle attached to a polyvinyl chloride-coated catheter (fastened to a 1 mL Luer-Lock™ syringe), the cisterna magna was carefully punctured. A slightly counterclockwise turn of the needle was made and approximately 100–120 μL of CSF was slowly aspirated through the catheter by aspirating the syringe. The collected CSF was transferred into 2 mL LoBind Eppendorf tubes. Immediately after CSF collection, 50 μL of collected CSF was mixed with 2.5 μL of PCA to ensure PDE deactivation. All CSF samples were kept on dry ice during sample collection, then stored frozen (−80 °C) until analysis. The detailed dosing scheme is shown in Table 2.

Male Carworth Farms (Crl:CF1 ®[CF-1]) mice (25–30 g) were obtained from CRL (Hollister, CA, US). The animals (n = 6/group) were dosed with the four inhibitors individually at 10 mg/kg each, or vehicle control, or all 4 inhibitors concomitantly at a dose of 10 mg/kg intraperitoneal (ip). Individual inhibitors and a cocktail of the four inhibitors were formulated in a mixture of 2% Tween-80: 0.5% CMC-Na at medium viscosity (MV). Half an hour after administration, the animals were sacrificed by brain-focused microwave irradiation (Muromachi MMW-05 with a WJR-28 water-jacketed mouse restrainer; 1.0 s at 5 kW). Microwave irradiated mice were then decapitated, and brain tissues were harvested with the dissection of the striatum following the same procedure as outlined for the rat. The mouse striatum is about 4–5 times smaller than the rat striatum. The striatum and the remainder of the brain tissues (including the brain stem and the cerebellum) were individually weighed and transferred to 1 mL cryotubes and placed on dry ice until the end of the procedure. Samples were then stored frozen (−80 °C) until bioanalysis.

2.3. Brain/striatum homogenate preparation

A 4-fold volume of 0.6 M PCA (for a 5-fold tissue dilution), and 2 stainless steel beads (MP Biomedicals, Solon, OH) were added to each pre-weighed tube containing rat or mouse brain or striatum tissues. The tissues were homogenized by using the FastPrep-24 5G kit (MP Biomedicals, Solon, OH) at a speed of 4.0 m/sec for 60 s. The rat or mouse brain homogenates were stored frozen (−80 °C) until analysis.

2.4. Determination of cAMP, cGMP and PDE inhibitor concentrations by LC—MS/MS

2.4.1. Brain/striatum homogenate sample processing

Fifty μL of striatum or brain tissue homogenates, calibration standards and quality control (QC) samples were mixed with 50 μL of 75:25 ACN/water, 50 μL of internal standard (IS) solution (50 ng/mL cIMP and 5 ng/mL carbamazepine in 0.6 M PCA) and 350 μL of mobile phase A (water containing 0.1% FA). The mixture was vortex-mixed for 5 min at room temperature and centrifuged at 1811 relative centrifugal force (rcf) for 10 min at a temperature of 10 °C. Supernatants (250 μL) were transferred to a 96-well plate for liquid chromatography tandem-mass spectrometry (LC—MS/MS) analysis. Striatum and brain tissue homogenate cAMP and cGMP concentrations were measured by LC—MS/MS using stable isotope-labeled cAMP and cGMP (eg, $^{13}C_5$-cAMP and $^{13}C^{15}N_2$-cGMP) as surrogate analytes to produce calibration curves in the brain tissue homogenate in the negative ionization mode. cIMP was used as the IS for both cAMP and cGMP. The PDE inhibitors were analyzed in the same run with the positive ionization mode alternating with the negative ionization mode for the determination of cNT levels. Carbamazepine was used as the IS for the measurements of all four PDE inhibitors. The standard curve ranged from 2 ng/mL to 2000 ng/mL for $^{13}C^{15}N_2$-cGMP and 5 ng/mL to 2000 ng/mL for $^{13}C_5$-cAMP and all four PDE inhibitors. Standard curves and QCs were prepared by the addition of spiking solutions into the rat brain homogenates (Chen et al., 2017). A dilution factor of 5-fold was used for all striatum and brain tissue homogenates to calculate tissue levels.

Table 2
Drug treatments for the rat and mouse studies (n = 6/group).

Study (species)	Group	Compound	Target	Dose (mg/kg)	Route	Euthanization Method	Sample Collected
A (rat)	1	Vehicle control			sc	Microwave Irradiation	Brain and Striatum
	2	DNS-0056	PDE1B	10			
	3	PF-05180999	PDE2A	10			
	4	PF-4447943	PDE9A	10			
	5	MP10	PDE10A	10			
	6	DNS-0056, PF-05180999, PF-4447943, MP10	Cocktail	10 each			
B (rat)	1	Vehicle control			sc	Anesthetic Overdose + Decapitation	CSF
	2	DNS-0056	PDE1B	10			
	3	PF-05180999	PDE2A	10			
	4	PF-4447943	PDE9A	10			
	5	MP10	PDE10A	10			
	6	DNS-0056, PF-05180999, PF-4447943, MP10	Cocktail	10 each			
C (rat)	1	Vehicle control			sc	Microwave Irradiation	Brain and Striatum
	2	DNS-0056	PDE1B	30			
	3	PF-05180999	PDE2A	30			
	4	PF-4447943	PDE9A	30			
	5	MP10	PDE10A	30			
D (mouse)	1	Vehicle control			ip	Microwave Irradiation	Brain and Striatum
	2	DNS-0056	PDE1B	10			
	3	PF-05180999	PDE2A	10			
	4	PF-4447943	PDE9A	10			
	5	MP10	PDE10A	10			
	6	DNS-0056, PF-05180999, PF-4447943, MP10	Cocktail	10 each			

2.4.2. CSF sample processing

Fifty μL of CSF samples (pre-treated with 2.5 μL PCA per 50 μL of CSF; see Section 2.2), calibration standards and QCs in artificial CSF were mixed with 50 μL of IS solution (50 ng/mL cIMP and 5 ng/mL carbamazepine in 0.6 M PCA) and 200 μL of mobile phase A (water containing 0.1% FA). Mixtures were vortex-mixed for 5 min at room temperature and centrifuged at 1811 rcf for 10 min at a temperature of 10 °C. Supernatants (200 μL) were transferred to a 96-well plate, covered with a silicone mat, and analyzed by LC–MS/MS. cAMP and cGMP concentrations in the CSF were measured by using cAMP and cGMP to produce calibration curves in the artificial CSF with cIMP as the IS. cAMP, cGMP and cIMP were acquired in negative ionization mode. In the same run, the PDE inhibitors were measured by using individual inhibitors to produce calibration curves in the artificial CSF with carbamazepine as the IS. PDE inhibitor and carbamazepine were acquired in positive ionization mode alternating with negative ionization mode used to detect the cNTs. The calibration curve ranged from 0.5 ng/mL to 200 ng/mL for cAMP and cGMP, and 0.5–2000 ng/mL for all four PDE inhibitors. Standard curves and QCs were prepared by the addition of spiking solutions into artificial CSF.

2.4.3. LC–MS/MS conditions for measuring cAMP, cGMP and the four PDE inhibitors

The LC–MS/MS method used was derived from a previous publication (Chen et al., 2017). Chromatographic separation was performed using a Waters Atlantis dc18, 3 μm, 3.0 × 100 mm column (Waters, Milford, MA) maintained at 40 °C. Mobile phase A consisted of water with 0.1% FA and mobile phase B consisted of ACN with 0.1% FA, delivered with Shimadzu Prominence LC-30AD pumps at a total flow rate of 1.2 mL/min with a back pressure less than 3800 psi. The gradient is shown in Table 2s. The column was interfaced to an AB SCIEX QTRAP 5500 (Foster City, CA, US) using a Turbo Spray ionization source operated in alternating positive and negative ionization modes. Scheduled multiple reaction monitoring (MRM) was used to scan the designed peaks at a 60 s window around the individual analytes' retention times to decrease mass spectrometry scan cycle time and thereby improve signal-to-noise ratios. The detailed scheduled MRM conditions are shown in Table 3s. The carryover of $^{13}C_5$-cAMP and $^{13}C^{15}N_2$-cGMP was accessed by injecting a matrix blank after the ULOQ standard. The data was acquired using Analyst software (v1.6.2) and processed with MultiQuant (v3.0.2) companion software (Applied Biosystems/MDS Sciex, Canada).

The levels of cAMP and/or cGMP in the inhibitor-dosed groups and the vehicle control groups were analyzed by an unpaired T-test assuming both populations have the same variability using GraphPad Prism software.

2.5. Stability of cAMP and cGMP in rat brain homogenate at room temperature

The rat brain tissues obtained following brain-focused microwave irradiation or cervical dislocation (non-microwaved, fresh rat brain) were added to a 4-fold volume of 0.1 M phosphate buffer solution (PBS, pH 7.4) (5-fold dilution) and 2 stainless steel beads. The brain tissues were homogenized using the FastPrep-24 5G with the conditions described above in Section 2.3. Fifty μL of the microwave-irradiated rat brain or fresh rat brain tissue homogenates were mixed with 950 μL of 0.1 M PBS (pH 7.4) to make 100-fold diluted brain tissue homogenates.

$^{13}C_5$-cAMP or $^{13}C^{15}N_2$-cGMP stock solutions were prepared in methanol-water (1:1) at a concentration of 10,000 ng/mL. Brain tissue homogenates from microwave-irradiated rat brain and fresh rat brain at dilutions of 5-fold and 100-fold were aliquoted to 96-well plates with

198 μL in each well. The stock solution (2 μL) was spiked in each well with 198 μL of brain tissue homogenate to achieve a final concentration of 100 ng/mL. The mixture was shaken at room temperature and quenched at 2, 5, 15 and 30 min with 800 μL of 0.6 M PCA-water. The control reference sample (time zero sample) was obtained immediately before spiking the stock solutions into the brain tissue homogenates. The concentrations of $^{13}C_5$-cAMP and $^{13}C^{15}N_2$-cGMP were measured by LC–MS/MS.

2.6. Rat CSF cAMP and cGMP room temperature stability verification procedures

$^{13}C_5$-cAMP or $^{13}C^{15}N_2$-cGMP, distinguished from endogenous cAMP or cGMP, were used to study their stability in rat CSF. $^{13}C_5$-cAMP or $^{13}C^{15}N_2$-cGMP stock solutions were prepared in methanol-water (1:1) at a concentration of 100 ng/mL. Fresh rat CSF (94 μL) obtained from the cisterna magna was mixed with 5 μL of either 0.1 M PBS (pH 7.4) or PCA. The mixture was spiked with 1 μL of $^{13}C_5$-cAMP or $^{13}C^{15}N_2$-cGMP stock solutions to make a final concentration of 1 ng/mL. The mixture was shaken at room temperature. 20 μL of the mixture was quenched at 0, 15, 30 and 60 min with 20 μL of 0.6 M PCA-water with IS (50 ng/mL cIMP). The mixture was vortex-mixed for 5 min and further mixed with 180 μL of mobile phase A (water containing 0.1% FA). Following the procedure described in Section 2.4, the concentration of $^{13}C_5$-cAMP and $^{13}C^{15}N_2$-cGMP were measured by LC–MS/MS.

3. Results

3.1. LC–MS/MS quantification of cAMP, cGMP and PDE inhibitors

LC–MS/MS methods were developed to analyze cAMP, cGMP and the PDE inhibitors in the same injection with the lowest limit of quantification (LLOQ) of 2 ng/mL for cAMP and 5 ng/mL for cGMP and PDE inhibitors in the brain; and of 0.5 ng/mL for cAMP/cGMP/PDE inhibitors in the CSF. The method carryover evaluated as the signal in matrix blank following the ULOQ standard was 1.5% of LLOQ for $^{13}C_5$-cAMP, 0.7% of LLOQ for $^{13}C^{15}N_2$-cGMP, which exceeded the FDA requirement that carry over should be less than 20% of LLOQ. In no case was carry over detected for the internal standard. A representative superimposed LC–MS/MS chromatogram is shown in Fig. 3.

3.2. Rat brain homogenate cAMP and cGMP room temperature stability verification results

At room temperature, both $^{13}C_5$-cAMP and $^{13}C^{15}N_2$-cGMP degrade rapidly in fresh brain tissue homogenates. With the dilution of the brain homogenate (less protein in the diluted homogenate) the rate of degradation slows down. The rate of degradation is faster for $^{13}C^{15}N_2$-cGMP than $^{13}C_5$-cAMP regardless of dilution. In fresh rat brain tissue homogenates (5-fold diluted with 0.1 M PBS [pH 7.4]), less than 1% of spiked $^{13}C^{15}N_2$-cGMP and about 5% of spiked $^{13}C_5$-cAMP were remaining following the 2-min incubation. In the higher diluted fresh rat brain tissue homogenates (100-fold diluted with 0.1 M PBS [pH 7.4]), less than 1% of spiked $^{13}C^{15}N_2$-cGMP was remaining while about 18% remaining of spiked $^{13}C_5$-cAMP following the 15-min incubation. Neither $^{13}C_5$-cAMP or $^{13}C^{15}N_2$-cGMP degrades in the microwave-irradiated brain homogenate (5-fold or 100-fold dilution in 0.1 M PBS [pH 7.4]) (Fig. 4).

3.3. Rat CSF cAMP and cGMP room temperature stability verification results

Spiked $^{13}C_5$-cAMP was stable in fresh rat CSF at room temperature for at least 1 h, while about 20% of spiked $^{13}C^{15}N_2$-cGMP degradated in 1 h. Pretreated rat CSF with 5% PCA (100 μL of CSF spiked with 5 μL of PCA) stops the degradation of $^{13}C^{15}N_2$-cGMP (Fig. 4).

3.4. Vehicle control group (baseline) cAMP and cGMP levels

In the vehicle control (NMP:PEG400:H_2O [10:40:50]) treated SD rats sacrificed by brain-focused microwave irradiation, the cAMP levels were 495 ng/g and 466 ng/g; the cGMP levels were 45.1 ng/g and 35.8 ng/g, in the brain and striatum, respectively. Neither cAMP or cGMP levels were statistically significantly different in rat brain or striatum. cGMP levels are about one-tenth of that of cAMP, which is consistent with the literature (Beavo and Brunton, 2002). The cAMP and cGMP levels in the CSF from vehicle control-treated rats were 7.79 ng/g and 2.01 ng/g, respectively (Fig. 5). The ratio of cAMP/cGMP in rat CSF is approximately 4, which is notably the same as the baseline cAMP/cGMP ratio in the CSF of patients with neuromuscular and neurological disorders (Brooks, 1980).

In the vehicle control (2% Tween-80: 0.5% CMC-Na, MV) treated CF-1 mice sacrificed by brain-focused microwave irradiation, the cAMP levels were 2330 ng/g in the brain and 1850 ng/g in the striatum; the cGMP levels were 20.1 ng/g in the brain and 11.3 ng/g in the striatum (Fig. 5). Similar to what was observed in the rats, neither cAMP or cGMP levels were statistically significantly different in mouse brain or striatum. Comparing the cAMP and cGMP levels in rat and mouse, the rat had higher cGMP levels, while the mouse had higher cAMP levels (Fig. 5).

3.5. Rat brain cNT changes following individual or concomitant PDE1B, PDE2A, PDE9A and PDE10A inhibitor administration

Generally, changes in cAMP levels compared to the vehicle control group were statistically insignificant in the rat CNS 1 h after either individual or concomitant administration of the studied PDE1B, PDE2A, PDE9A and PDE10A inhibitors at a dose of 10 mg/kg or 30 mg/kg (Fig. 6).

Following administration of PDE2A, PDE9A or PDE10A inhibitors at

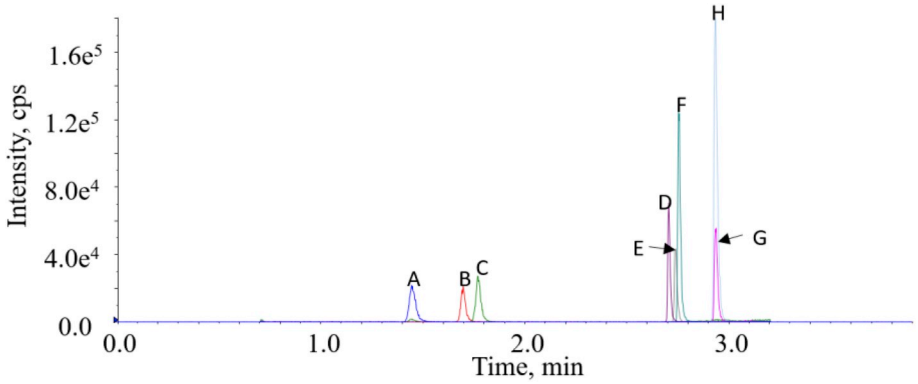

Fig. 3. A superimposed LC–MS/MS chromatogram of cAMP and cGMP, four PDE inhibitors and internal standards. A: cAMP; B: cGMP; C: cIMP (IS) were acquired in negative ionization mode; D: PF-4447943; E: DNS-0056; F: MP10; G: PF-05180999; H: Carbamazepine (IS) were acquired in positive ionization mode. The concentration of carbamazepine was 0.5 ng/mL, cIMP and the rest of the analytes were 5 ng/mL in 0.1% FA with 5% ACN.

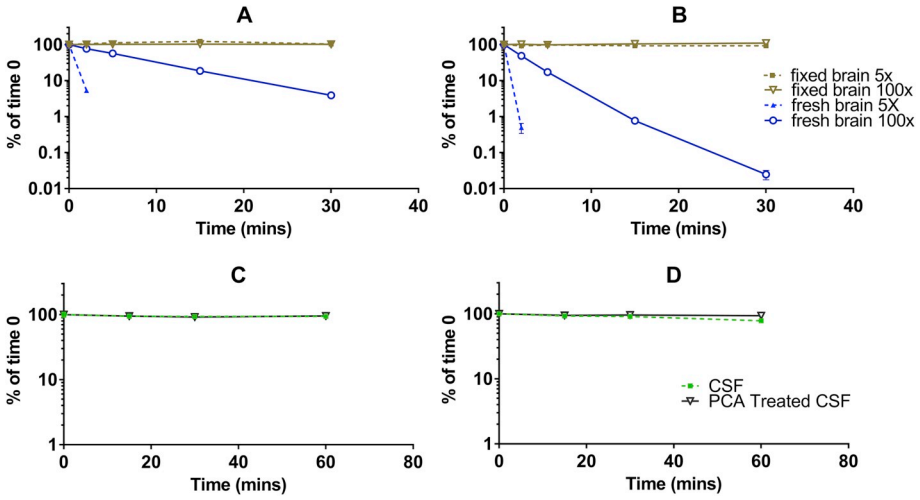

Fig. 4. Stability of $^{13}C_5$-cAMP and $^{13}C^{15}N_2$-cGMP in microwave-fixed rat brain (vs. fresh brain) and in PCA-treated CSF (vs. untreated CSF). $^{13}C^5$-cAMP (A) or $^{13}C^{15}N_2$-cGMP (B) were spiked in rat brain homogenates (5-fold and 100-fold dilution in 0.1 M PBS [pH 7.4]) at a final concentration of 100 ng/mL (n = 3/timepoint). The mixture was placed at room temperature and quenched with 0.6 M PCA at 0, 2, 5, 15 and 30 min. Both $^{13}C^5$-cAMP and $^{13}C^{15}N_2$-cGMP disappeared rapidly in fresh rat brain homogenates with either 5-fold or 100-fold dilution with 0.1 M PBS (pH 7.4), but stable in microwave irradiated rat brain homogenates with either 5-fold or 100-fold dilution with 0.1 M PBS (pH 7.4). $^{13}C_5$-cAMP (C) or $^{13}C^{15}N_2$-cGMP (D) were spiked in fresh rat CSF at a final concentration of 1 ng/mL (n = 3/timepoint). The mixture was placed at room temperature and quenched with 0.6 M PCA at 0, 15, 30 and 60 min $^{13}C_5$-cAMP was stable in the CSF, while about 20% of $^{13}C^{15}N_2$-cGMP disappeared in CSF in 60 min. Both $^{13}C_5$-cAMP and $^{13}C^{15}N_2$-cGMP were stable in PCA pretreated CSF.

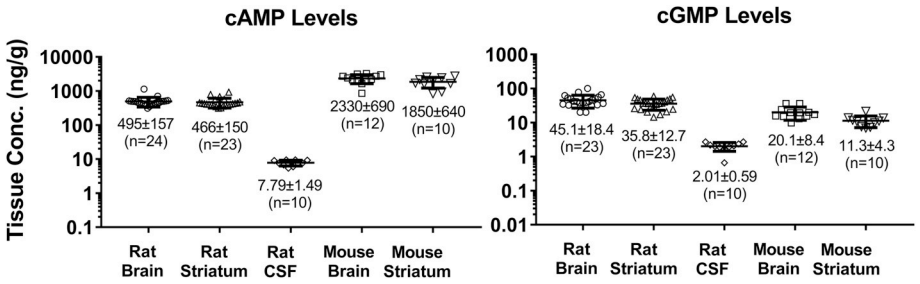

Fig. 5. cAMP and cGMP levels (ng/g) in rat and mouse brain/striatum tissues and in rat CSF (the animals were treated with vehicle). Values are mean ± SD. Brain and striatum samples from male Sprague Dawley rat or male CF-1 mice were collected after microwave irradiation; rat CSF was collected from the cisterna magna under isoflurane anesthesia. The collected CSF was immediately mixed with PCA (50 μL of CSF + 2.5 μL of PCA).

a dose of 10 or 30 mg/kg, cGMP levels increased in the rat CNS. 10 mg/kg administration of a PDE2A inhibitor (PF-05180999) sc lead to increased cGMP levels in rat brain, striatum and CSF (2.0-fold, 2.2-fold and 1.5-fold, respectively) over the vehicle control-treated animals. A higher dose of PF-05180999 (30 mg/kg) resulted in a higher increase in both brain and striatum cGMP (3.6-fold over vehicle control group) levels compared with animals treated at 10 mg/kg. Following a 10 mg/kg sc dose of a PDE9A inhibitor (PF-4447943), cGMP increases over vehicle control were only observed in rat CSF (2.2-fold). Additionally, following administration of a 30 mg/kg dose, cGMP increases over vehicle control were observed in both brain and striatum (1.8-fold and 2.2-fold, respectively). Administration of a 10 mg/kg dose of PDE10A inhibitor (MP10) did not result in any changes in cGMP levels compared with vehicle control group. Increasing the dose to 30 mg/kg, however, resulted in an increased level of cGMP in the striatum (1.7-fold) (Fig. 6). No cGMP increase was observed following PDE1B inhibitor (DNS-0056) dosing.

Following concomitant dosing of the four inhibitors at a dose of 10 mg/kg each, cGMP increases over vehicle control were observed in the rat brain, striatum and CSF (3.3-fold, 4.4-fold and 2.9-fold, respectively). However, the inhibitor exposures by dosing the four PDE inhibitors concomitantly were higher (within 1-fold to approximately 3-fold depending on the individual inhibitors) in comparison to dosing them individually (Table 3).

cAMP and cGMP changes versus vehicle control also generally followed a similar trend in the rat brain, striatum and CSF (Fig. 6) after PDE inhibitors administration.

3.6. Mouse brain cAMP and cGMP changes following PDE1B, PDE2A, PDE9A and PDE10A inhibitor dosing at a dose of 10 mg/kg

Similar to the observations in the rat, cAMP changes versus a vehicle control in the mouse CNS were minor after individual dosing of PDE1B, PDE2A, PDE9A and PDE10A inhibitors at a dose of 10 mg/kg each (Fig. 7).

cGMP changes were observed in the mouse CNS after PDE2A, PDE9A and PDE10A individual inhibitor dosing. Following 10 mg/kg administration of PDE2 inhibitor (PF-05180999), cGMP level increased in the mouse brain and striatum (3.9-fold and 6.4-fold, respectively) compared to the vehicle control group. Following 10 mg/kg administration of PDE9 inhibitor (PF-4447943), cGMP increases over vehicle control were also observed in the mouse brain and striatum (2.0-fold and 2.8-fold, respectively). Administration of 10 mg/kg of PDE10 inhibitor (MP10), resulted in a 1.7-fold cGMP increase over vehicle control in striatum, but not in the brain tissue. Following administration of 10 mg/kg of PDE1 inhibitor (DNS-056), cGMP level decreased (0.6-fold) in the mouse brain compared to vehicle treated control group.

After concomitant dosing of the PDE1B, PDE2A, PDE9A and PDE10A inhibitors at 10 mg/kg each, prominent cGMP increases over vehicle control were observed in the mouse brain and striatum (18-fold and 36.7-fold, respectively). cAMP increases over vehicle control were observed in the striatum (1.6-fold). This is the only time cAMP increases were observed in this set of studies. The drug exposures by dosing the four PDE inhibitors concomitantly were higher (within 2-fold to approximately 7-fold depending on the individual inhibitors) in comparison to individual inhibitor dosing (Table 4).

4. Discussion

Local cNT changes have been proposed as a biomarker for PDE inhibition (Mirone et al., 2009; Nicholas et al., 2009). Since the degradation of cNTs by PDEs is rapid and does not require any cofactors, sample processing for accurate cNT measurement is challenging. To accurately measure cNT levels in the tissues, a rapid tissue-fixation method is needed. The sample processing procedure for accurate cNT

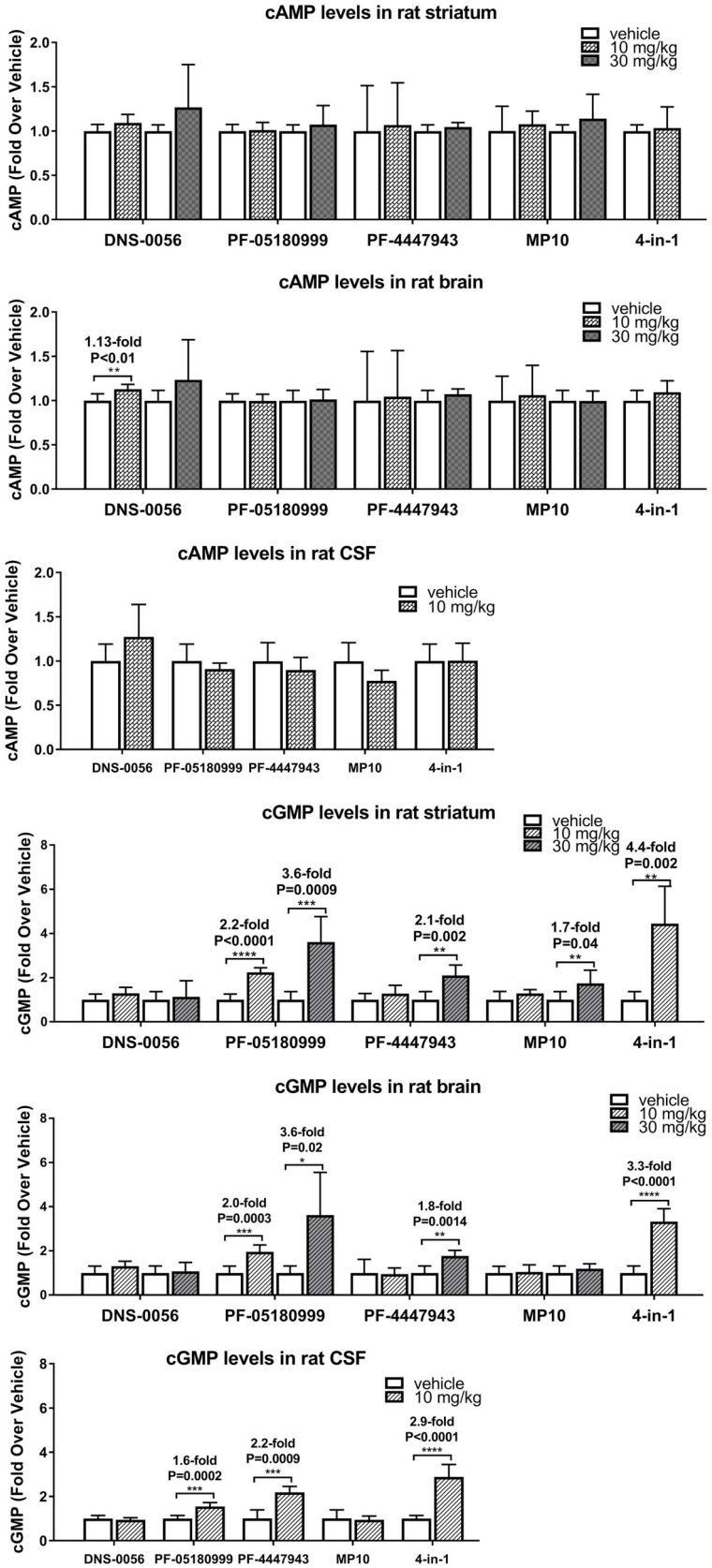

Fig. 6. cNT fold increase over vehicle control group in rat brain, striatum and CSF 1 h after subcutaneous administration of DNS-0056 (PDE1B), PF-05180999 (PDE2A), PF-4447943 (PDE9A), and MP10 (PDE10A) at 10 mg/kg and 30 mg/kg or subcutaneous concomitant administration of the four inhibitors at a dose of 10 mg/kg each (n = 6/group).

Table 3
PDE inhibitor concentrations in rat brain, striatum and CSF 1 h after individual PDE1B, PDE2A, PDE9A, and PDE10A inhibitor subcutaneous administration (10 or 30 mg/kg) or concomitant subcutaneous administration of the four inhibitors (10 mg/kg each inhibitor) (n = 6/group).

	Mean ± SD (ng/g or mL[a])	DNS-0056 (PDE1B)	PF-05180999 (PDE2A)	PF-4447943 (PDE9A)	MP10 (PDE10A)
10 mg/kg Individual Dosing	Brain	1510 ± 365	565 ± 159	650 ± 290	204 ± 117
	Striatum	1710 ± 457	597 ± 131	565 ± 196	296 ± 139
	CSF	38.4 ± 11.2	209 ± 63.9	674 ± 187	4.21 ± 2.59
10 mg/kg Concomitant Dosing	Brain	1610 ± 634	712 ± 323	877 ± 340	692 ± 252
	Striatum	1630 ± 660	761 ± 296	823 ± 334	855 ± 260
	CSF	43.4 ± 12.4	331 ± 114	763 ± 264	2.07 ± 0.59
30 mg/kg Individual Dosing	Brain	2080 ± 473	1790 ± 593	1960 ± 292	756 ± 335
	Striatum	1740 ± 459	1580 ± 475	1840 ± 274	749 ± 154

Values are mean ± SD.
[a] The unit is ng/g for brain and striatum samples; ng/mL for CSF samples.

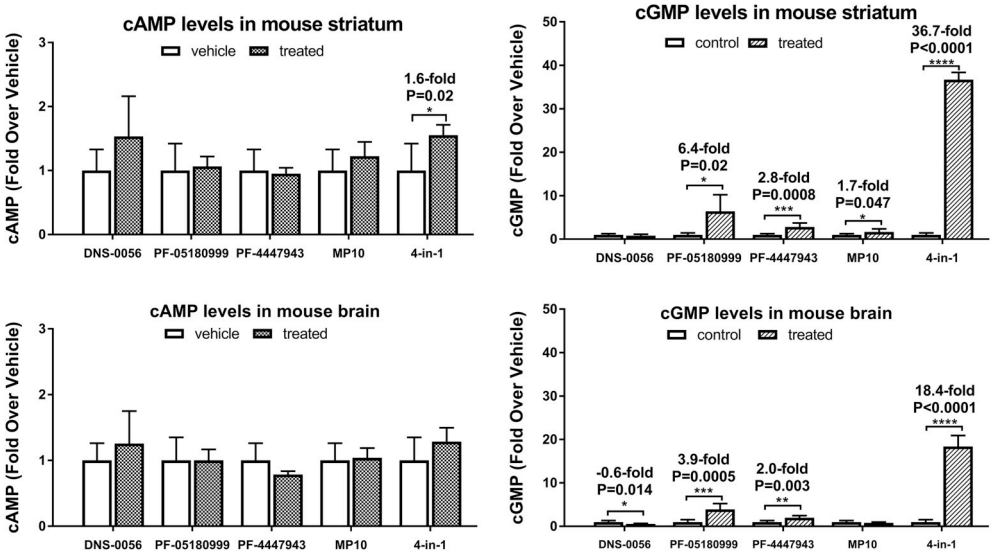

Fig. 7. cNT fold increase over vehicle control group in mouse brain and striatum 0.5-h after DNS-0056 (PDE1B), PF-05180999 (PDE2A), PF-4447943 (PDE9A), and MP10 (PDE10A) intraperitoneal administration at 10 mg/kg or concomitant intraperitoneal administration of the four inhibitors at a dose of 10 mg/kg (n = 6/group).

measurement has evolved from rapid tissue freezing in liquid nitrogen or carbon dioxide to microwave irradiation (Pauk and Reddy, 1967; Steiner et al., 1969). Our studies show that spiked $^{13}C_5$-cAMP and $^{13}C^{15}N_2$-cGMP remains stable in the microwave-irradiated rat brain homogenates, but not in unfixed homogenates (Fig. 4). Although the degradation of spiked $^{13}C_5$-cAMP or $^{13}C^{15}N_2$-cGMP is much slower in rodent CSF relative to degradation rates in rat brain tissue homogenates, we pretreated rat CSF with PCA to completely prevent the degradation of cNTs in the CSF (Fig. 4).

In addition to sample processing optimization, a LC–MS/MS method was developed to analyze cNTs and PDE inhibitors with moderate throughput. In this method, to minimize the interference of endogenous components, a negative ionization mode was used to detect cAMP/cGMP levels. In addition, a positive ionization mode was used to measure PDE inhibitor concentrations; scheduled MRM was used to program the MRM near the analytes' retention times to improve sensitivity. To overcome the interference of endogenous cNTs, artificial CSF was used as surrogate matrix for cNT analysis in CSF; stable-labeled cAMP/cGMP were used as surrogate analyte standards to produce calibration curves in the brain matrix. Compared with the traditional ELISA method, LS-MS/MS method is specific, with higher throughput and wider linear range. The cNT baseline levels measured are consistent with reported literature values (Suzuki et al., 2015).

Although PDE1, PDE2 and PDE10 metabolize both cAMP and cGMP, individually, PDE1B, PDE2A and PDE10A inhibition did not result in statistically significant CNS cAMP changes in most of our studies in both mouse and rat. Increases in cGMP levels were observed with dose-dependent increases following PDE2A, PDE9A and PDE10A inhibition up to 30 mg/kg. DNS-0056 (PDE1B inhibitor) administration did not cause statistically significant CNS cGMP changes. The lack of cGMP increase may be due to the potency of the selected PDE1B inhibitor. After testing a more potent, in-house PDE1B inhibitor, statistically significant cGMP increases were observed (unpublished observations). These data indicate cGMP is a more suitable pharmacokinetic

Table 4
PDE inhibitor concentrations (ng/g) in mouse striatum or brain 0.5-h after individual PDE1B, PDE2A, PDE9A, and PDE10A inhibitor intraperitoneal administration (10 mg/kg) or concomitant administration of PDE1B, 2A, 9A and 10A inhibitors (10 mg/kg each inhibitor) (n = 6/group).

	Mean ± SD (ng/g)	DNS-0056 (PDE1B)	PF-05180999 (PDE2A)	PF-4447943 (PDE9A)	MP10 (PDE10A)
10 mg/kg Individual Dosing	Striatum	967 ± 316	1520 ± 432	2440 ± 692	1320 ± 386
	Brain	1060 ± 343	1680 ± 500	2990 ± 526	1810 ± 473
10 mg/kg Concomitant Dosing	Striatum	7960 ± 1070	3520 ± 384	6360 ± 703	3180 ± 316
	Brain	7110 ± 947	3770 ± 556	6050 ± 925	2280 ± 332

Values are mean ± SD.

biomarker for CNS PDE inhibition. cAMP has a relatively slower degradation rate and much higher baseline levels than that of cGMP, therefore, the cAMP increases after PDE inhibition are masked by their higher background levels.

Preclinically, rat and mouse are the preferred animal models most commonly utilized to detect cNT changes after dosing PDE inhibitors. The selection of rat or mouse usually depends upon the established preclinical efficacy model. There were no observed changes for cAMP levels after administration of PDE1B, PDE2A, PDE9A or PDE10A inhibitors to male SD rats or male CF-1 mice at a dose of 10 mg/kg. In contrast, an increase in cGMP levels was observed following administration of PDE inhibitors in both rat and mouse. Notably, cGMP changes followed the same trend in the rat and mouse CNS, however, the magnitude of the cGMP changes versus vehicle control were higher in the mouse compared to the rat CNS. In addition to species differences, the observed higher cGMP increase in mouse may be associated with a higher PDE inhibitor exposure in the mouse than in the rat (Table 4).

Since CSF is not rich in PDEs (or proteins in general), it may serve as a collection reservoir for circulating cNTs within the CNS and therefore may be a useful tissue with which to monitor cNT changes. Although PDE activity has been found in CSF (Hidaka et al., 1975), it is relatively low in comparison to the brain tissue (which is very rich in PDEs), resulting in much slower degradation of the cNTs present compared to those of the brain (Fig. 4). In this study, after PDE inhibition, the same trend was observed for cNT changes in the brain, striatum and CSF samples. Bearing in mind the considerable effort associated with microwave irradiation of the animals, brain tissue collection, and striatum dissection, it is clearly much easier to collect CSF for cNT level determination. The cGMP level change in CSF has been reported as a biomarker of PDE9 inhibition (Nicholas et al., 2009). Our data shows that concentrations of cGMP in the CSF could also be used as a biomarker for other PDEs that modulate cGMP.

Our lab has found the dose required to observe cGMP level increases in the CNS after PDE2A, PDE9A, or PDE10A inhibitor administration is at least 10 mg/kg for both mouse and rat, which is a magnitude higher than the dose required to observe efficacy (usually less than 1 mg/kg in the NOR model). It is reasonable to speculate that changes in regional cGMP levels within cellular microcompartments, which are directly linked to efficacy, are higher than the levels detected in the tissue homogenates. It is generally accepted that the modulation of cNT concentrations within specific microcompartments are associated with pharmacodynamics and efficacy (Arora et al., 2013). Current technology such as FRET can detect the cNTs within microenvironments, but it is challenging to accurately quantify them in these specific tissue locations (Zaccolo, 2006; Zaccolo et al., 2000). Practically, we can only measure cNT concentrations within the bulk tissue homogenates and those results therefore can only serve as an approximation of the concentration at the target. The temporal and spatial cNT concentrations within the microcompartment associated with target engagement and efficacy, could potentially be magnitudes higher than the cNT concentrations in the tissue homogenates. This may explain why a higher dose is required to observe tissue cNT changes rather than the dose required to observe efficacy. Nonetheless, cNT tissue concentrations are useful as an indicator for PDE inhibition (Mirone et al., 2009). The tissue with high PDE expression such as striatum, is more sensitive to PDE inhibition and this could be an ideal target to monitoring cNT changes.

Although the absorption, brain uptake and elimination of the four inhibitors differ for the four inhibitors tested in this study, we selected 1 h time point for rat and 0.5 h time point for mouse, which is close to the T_{max} of those individual inhibitors after a single sc or ip dose of 10 mg/kg. The brain concentrations of the inhibitors, which affected by absorption, brain uptake, elimination and efflux components, is monitored. At a dose of 10 mg/kg, the free brain concentration of the tested inhibitors are magnitudes higher than IC_{50} across all 4 PDE inhibitors. Based on the biology of PDE inhibition and subsequent cAMP/cGMP increase, a direct response model was expected. In this case, inhibitor concentrations in the target we measured, are directly responsible for the pharmacodynamic response (cAMP/cGMP levels) being measured.

PDE1, PDE2, PDE9 and PDE10 are the four PDEs that degrade cGMP and are expressed in brain. A simultaneous inhibition of these 4 PDE isoenzymes resulted in a prominent increased CNS cGMP level. Similarly, if we inhibit all the PDE isoenzymes expressed in the brain that degrade cAMP (PDE4, PDE7, PDE1, PDE2 and PDE10) simultaneously, an increased cAMP levels would be expected (Fig. 1). Unfortunately, currently, there is no potent PDE7 inhibitor with appropriate pharmacokinetics. An alternative experiment is to stimulate the production of cAMP or cGMP while inhibiting their degradation through administration of PDEs inhibitors. Given the fact that the rate of cNT synthesis by cyclase is much slower than their degradation by PDEs (Beavo and Brunton, 2002; Schmidt, 2010), PDE inhibition is the dominant approach to regulate cNT levels.

Synergistic effects among different PDE inhibitors, either in vivo or in vitro, appear in the literature (Kraynik et al., 2013; Schermuly et al., 1999), though little information can be found about the inhibitor concentrations after coadministration. Accordingly, we propose that synergistic effects may be operative with the PDE inhibitor levels examined this study. PDE1, PDE2, PDE9 and PDE10 are the PDEs in the brain that use cGMP as a substrate. After orally dosing PDE1B, PDE2A, PDE9A and PDE10A inhibitors concomitantly at 10 mg/kg each to male SD rats or male CF-1 mice, the cGMP increase was much more pronounced as compared to individual inhibitor dosing (Figs. 6 and 7). The inhibitor concentrations were also higher after concomitant dosing compared with individual inhibitor dosing (Table 3, Table 4). It is not fully understood whether the observed effect of concomitant dosing is a result of synergy or simply a result of increased inhibitor concentration.

cNTs have been extensively studied over the past half century and PDEs are of keen interest to the pharmaceutical industry as potential drug development targets. In this work, we explored a proof of concept approach for early screening to evaluate cNT modulation due to PDE inhibition. To that end, a standard method for sample collection, processing and detection of cNT modulation is necessary. The reported cNT levels in the literature are variable likely due to uncontrolled degradation or metabolism and/or because of different measurement methods. In addition, little has been reported regarding species dependence, brain-regional distribution, and synergistic effect in cNT level changes after PDE inhibitor treatment. Following optimization and validation of the sample processing and detection methods, we systematically studied the species difference of cNT concentrations in the mouse and rat in response to PDE inhibition. Differences in the regional response of cNT changes in striatum, CSF, and the rest of the brain were also evaluated in rats and mice. The information obtained from this study should lead to an improved design for future preclinical studies, aimed at detecting cNT changes that occur following PDE inhibition.

Acknowledgements

We would like to acknowledge Guibao Gu and Yu-Wen Li for providing technical guidance on brain tissue dissection and microwave fixation specifications; Scott Silveria for providing technical assistance on physicochemical properties calculation using CDD Vault.

This research did not receive any specific grant from funding agencies in the public, commercial, or non-profit sectors.

Appendix A. Supplementary data

Supplementary data to this article can be found online at https://doi.org/10.1016/j.neuint.2019.104471.

References

Ahmad, F., Murata, T., Shimizu, K., Degerman, E., Maurice, D., Manganiello, V., 2015. Cyclic nucleotide phosphodiesterases: important signaling modulators and therapeutic targets. Oral Dis. 21, e25–50.

Arora, K., Sinha, C., Zhang, W., Ren, A., Moon, C.S., Yarlagadda, S., Naren, A.P., 2013. Compartmentalization of cyclic nucleotide signaling: a question of when, where, and why? Pflügers Archiv 465, 1397–1407.

Beavo, J.A., Brunton, L.L., 2002. Cyclic nucleotide research – still expanding after half a century. Nat. Rev. Mol. Cell Biol. 3, 710–718.

Brooks, B.R., Wood, J.H., Diaz, M., Czerwinski, C., Georges, L.P., Sode, J., Ebert, M.H., Engel, W.K., 1980. Extracellular cyclic nucleotide metabolism in the human central nervous system. In: Wood, J.H. (Ed.), Neurobiology of Cerebrospinal Fluid 1. Plenum Press, pp. 113–139.

Chen, J., Tabatabaei, A., Zook, D., Wang, Y., Danks, A., Stauber, K., 2017. A surrogate analyte-based liquid chromatography-tandem mass spectrometry method for the determination of endogenous cyclic nucleotides in rat brain. J. Pharm. Biomed. Anal. 146, 361–368.

Dyck, B., Branstetter, B., Gharbaoui, T., Hudson, A.R., Breitenbucher, J.G., Gomez, L., Botrous, I., Marrone, T., Barido, R., Allerston, C.K., Cedervall, E.P., Xu, R., Sridhar, V., Barker, R., Aertgeerts, K., Schmelzer, K., Neul, D., Lee, D., Massari, M.E., Andersen, C.B., Sebring, K., Zhou, X., Petroski, R., Limberis, J., Augustin, M., Chun, L.E., Edwards, T.E., Peters, M., Tabatabaei, A., 2017. Discovery of selective phosphodiesterase 1 inhibitors with memory enhancing properties. J. Med. Chem. 60, 3472–3483.

Evellin, S., Mongillo, M., Terrin, A., Lissandron, V., Zaccolo, M., 2004. Measuring dynamic changes in cAMP using fluorescence resonance energy transfer. Methods Mol. Biol. 284, 259–270.

Grauer, S.M., Pulito, V.L., Navarra, R.L., Kelly, M.P., Kelley, C., Graf, R., Langen, B., Logue, S., Brennan, J., Jiang, L., Charych, E., Egerland, U., Liu, F., Marquis, K.L., Malamas, M., Hage, T., Comery, T.A., Brandon, N.J., 2009. Phosphodiesterase 10A inhibitor activity in preclinical models of the positive, cognitive, and negative symptoms of schizophrenia. J. Pharmacol. Exp. Ther. 331, 574–590.

Helal, C.J., Arnold, E.P., Boyden, T.L., Chang, C., Chappie, T.A., Fennell, K.F., Forman, M.D., Hajos, M., Harms, J.F., Hoffman, W.E., Humphrey, J.M., Kang, Z., Kleiman, R.J., Kormos, B.L., Lee, C.W., Lu, J., Maklad, N., McDowell, L., Mente, S., O'Connor, R.E., Pandit, J., Piotrowski, M., Schmidt, A.W., Schmidt, C.J., Ueno, H., Verhoest, P.R., Yang, E.X., 2017. Application of structure-based design and parallel chemistry to identify a potent, selective, and brain penetrant phosphodiesterase 2A inhibitor. J. Med. Chem. 60, 5673–5698.

Hidaka, H., Shibuya, M., Asano, T., Hara, F., 1975. Cyclic nucleotide phosphodiesterase of human cerebrospinal fluid. J. Neurochem. 25, 49–53.

Ke, H., Wang, H., Ye, M., 2011. Structural insight into the substrate specificity of phosphodiesterases. Handb. Exp. Pharmacol. 121–134.

Kelly, M.P., Adamowicz, W., Bove, S., Hartman, A.J., Mariga, A., Pathak, G., Reinhart, V., Romegialli, A., Kleiman, R.J., 2014. Select 3',5'-cyclic nucleotide phosphodiesterases exhibit altered expression in the aged rodent brain. Cell. Signal. 26, 383–397.

Keravis, T., Lugnier, C., 2012. Cyclic nucleotide phosphodiesterase (PDE) isozymes as targets of the intracellular signalling network: benefits of PDE inhibitors in various diseases and perspectives for future therapeutic developments. Br. J. Pharmacol. 165, 1288–1305.

Kleiman, R.J., Chapin, D.S., Christoffersen, C., Freeman, J., Fonseca, K.R., Geoghegan, K.F., Grimwood, S., Guanowsky, V., Hajos, M., Harms, J.F., Helal, C.J., Hoffmann, W.E., Kocan, G.P., Majchrzak, M.J., McGinnis, D., McLean, S., Menniti, F.S., Nelson, F., Roof, R., Schmidt, A.W., Seymour, P.A., Stephenson, D.T., Tingley, F.D., Vanase-Frawley, M., Verhoest, P.R., Schmidt, C.J., 2012. Phosphodiesterase 9A regulates central cGMP and modulates responses to cholinergic and monoaminergic perturbation in vivo. J. Pharmacol. Exp. Ther. 341, 396–409.

Kraynik, S.M., Miyaoka, R.S., Beavo, J.A., 2013. PDE3 and PDE4 isozyme-selective inhibitors are both required for synergistic activation of brown adipose tissue. Mol. Pharmacol. 83, 1155–1165.

Megens AAHP, Langlois XJM, Vanhoof GCP, ANDRÉS-GIL JI, De AM, Buijnsters PJJA, TRABANCO-SUÁREZ AA, Rombouts FJR. Combinations comprising pde 2 inhibitors such as 1-aryl-4-methyl- [1,2,4] triazolo [4,3-a] Quinoxaline Compounds and Pde 10 Inhibitors for Use in the Treatment of Neurological or Metabolic Disorders. Google Patents, 2014.

Menniti, F.S., Faraci, W.S., Schmidt, C.J., 2006. Phosphodiesterases in the CNS: targets for drug development. Nat. Rev. Drug Discov. 5, 660–670.

Mirone, V., d'Emmanuele di Villa Bianca, R., Mitidieri, E., Imbimbo, C., Fusco, F., Verze, P., Vitale, D.F., Sorrentino, R., Cirino, G., 2009. Platelet cyclic guanosine monophosphate as a biomarker of phosphodiesterase type 5 inhibitor efficacy in the treatment of erectile dysfunction: a randomized placebo-controlled study. Eur. Urol. 56, 1067–1073.

Nicholas, T., Evans, R., Styren, S., Qiu, R., Wang, E.Q., Nelson, F., Grimwood, V.L., Sarah, Christoffersen C., Banerjee, S., Corrigan, B., Kocan, G., Geoghegan, K., Carrieri, C., Raha, N., Verhoest, P., Soares, H., 2009. PF-04447943, a novel PDE9A inhibitor, increases cGMP levels in cerebrospinal fluid: translation from non-clinical species to healthy human volunteers. In: Alzheimer's Association International Conference on Alzheimer's Disease (ICAD): Vienna, Austria, P330–P1.

Oeckl, P., Steinacker, P., Lehnert, S., Jesse, S., Kretzschmar, H.A., Ludolph, A.C., Otto, M., Ferger, B., 2012. CSF concentrations of cAMP and cGMP are lower in patients with Creutzfeldt-Jakob disease but not Parkinson's disease and amyotrophic lateral sclerosis. PLoS One 7, e32664.

Pauk, G.L., Reddy, W.J., 1967. Measurement of adenosine 3',5'-monophosphate. Anal. Biochem. 21, 298–307.

Schermuly, R.T., Ghofrani, H.A., Enke, B., Weissmann, N., Grimminger, F., Seeger, W., Schudt, C., Walmrath, D., 1999. Low-dose systemic phosphodiesterase inhibitors amplify the pulmonary vasodilatory response to inhaled prostacyclin in experimental pulmonary hypertension. Am. J. Respir. Crit. Care Med. 160, 1500–1506.

Schmidt, C.J., 2010. Phosphodiesterase inhibitors as potential cognition enhancing agents. Curr. Top. Med. Chem. 10, 222–230.

Steiner, A.L., Kipnis, D.M., Utiger, R., Parker, C., 1969. Radioimmunoassay for the measurement of adenosine 3',5'-cyclic phosphate. Proc. Natl. Acad. Sci. U. S. A. 64, 367–373.

Suzuki, K., Harada, A., Shiraishi, E., Kimura, H., 2015. In vivo pharmacological characterization of TAK-063, a potent and selective phosphodiesterase 10A inhibitor with antipsychotic-like activity in rodents. J. Pharmacol. Exp. Ther. 352, 471–479.

Zaccolo, M., 2006. Phosphodiesterases and compartmentalized cAMP signalling in the heart. Eur. J. Cell Biol. 85, 693–697.

Zaccolo, M., De Giorgi, F., Cho, C.Y., Feng, L., Knapp, T., Negulescu, P.A., Taylor, S.S., Tsien, R.Y., Pozzan, T., 2000. A genetically encoded, fluorescent indicator for cyclic AMP in living cells. Nat. Cell Biol. 2, 25–29.

Unresolved References

Brooks, B.R., Wood, J.H., Diaz, M., Czerwinski, C., Georges, L.P., Sode, J., Ebert, M.H., Engel, W.K., 1980. Extracellular cyclic nucleotide metabolism in the human central nervous system. In: Wood, J.H. (Ed.), Neurobiology of Cerebrospinal Fluid 1. Plenum Press, pp. 113–139.

Megens, A.A.H.P., Langlois, X.J.M., Vanhoof, G.C.P., ANDRÉS-GIL, J.I., De, A.M., Buijnsters, P.J.J.A., TRABANCO-SUÁREZ, A.A., Rombouts, F.J.R., 2014. Combinations comprising pde 2 inhibitors such as 1-aryl-4-methyl- [1,2,4] triazolo [4,3-a] quinoxaline compounds and pde 10 inhibitors for use in the treatment of neurological or metabolic disorders,Google Patents.

Nicholas, T., Evans, R., Styren, S., Qiu, R., Wang, E.Q., Nelson, F., Grimwood, V.L., Sarah, Christoffersen, C., Banerjee, S., Corrigan, B., Kocan, G., Geoghegan, K., Carrieri, C., Raha, N., Verhoest, P., Soares, H., 2009. PF-04447943, a novel PDE9A inhibitor, increases cGMP levels in cerebrospinal fluid: translation from non-clinical species to healthy human volunteers. In: Alzheimer's Association International Conference on Alzheimer's Disease (ICAD). Vol. 5. pp. P330–P331 Vienna, Austria.